

# Novel High-Temperature Fiber-Optic Pressure Sensor Based on Etched PCF F-P Interferometer Micromachined by a 157-nm Laser

Zengling Ran, *Member, IEEE*, Shan Liu, Qin Liu, Yanjun Wang, Haihong Bao, and Yunjiang Rao, *Member, IEEE*

**Abstract**—A self-enclosed fiber-optic Fabry–Perot (F–P) cavity is created by splicing a single-mode fiber to a photonic crystal fiber (PCF) with a precise hole micromachined by a 157-nm laser at the end face of the PCF. Furthermore, such a F–P cavity is etched chemically and its high-temperature and pressure responses are investigated experimentally. The pressure sensitivity is  $\sim 54.7$  pm/MPa and the temperature sensitivity is  $\sim 0.45$  pm/°C. The proposed sensor could offer some excellent features such as good high-temperature stability, low cross-sensitivity between pressure and temperature, ease of mass-production, making it attractive for pressure measurement under high-temperature.

**Index Terms**—Fiber-optic pressure sensor, photonic crystal fiber, laser micro-machining, high temperature.

## I. INTRODUCTION

FIBER-OPTIC Fabry–Perot interferometer (FPI) sensors have been attracting much interest because they offer many outstanding advantages, such as high sensitivity, high temperature survivability, compact size, corrosion resistance, and immunity to electromagnetic interference [1]. These advantages make them suitable for deployment in space-limited harsh environments such as high-speed wind tunnels, turbine engines, power plants and oil and gas down-hole exploration, where pressure is one of the important measurands [2]–[7].

Many methods have been developed to fabricate fiber optic FPIs. These include using conventional hollow-core

Manuscript received July 16, 2014; revised September 25, 2014; accepted October 30, 2014. Date of publication December 8, 2014; date of current version May 19, 2015. This work was supported in part by the National Natural Science Foundation of China under Grant 51205049, in part by the Program for Changjiang Scholars and Innovative Research Team in University under Grant IRT1218, in part by the 111 Project under Grant B14039, in part by the Major Equipment Projects through the Ministry of Science and Technology under Grant M1701010112YQ2500213, and in part by the Program for New Academic Men Award, University of Electronic Science and Technology of China, Chengdu, China, under Grant Y03001023601017010. The associate editor coordinating the review of this paper and approving it for publication was Dr. Hsiao-Wen Zan.

The authors are with the Key Laboratory of Optical Fiber Sensing and Communications, Ministry of Education, University of Electronic Science and Technology of China, Chengdu 610051, China (e-mail: ranzl@uestc.edu.cn; 742791715@qq.com; ccliug@gmail.com; 504058586@qq.com; edwardbao@sina.cn; yjrao@uestc.edu.cn).

Color versions of one or more of the figures in this paper are available online at <http://ieeexplore.ieee.org>.

Digital Object Identifier 10.1109/JSEN.2014.2371243

1530-437X © 2014 IEEE. Personal use is permitted, but republication/redistribution requires IEEE permission. See [http://www.ieee.org/publications\\_standards/publications/rights/index.html](http://www.ieee.org/publications_standards/publications/rights/index.html) for more information.

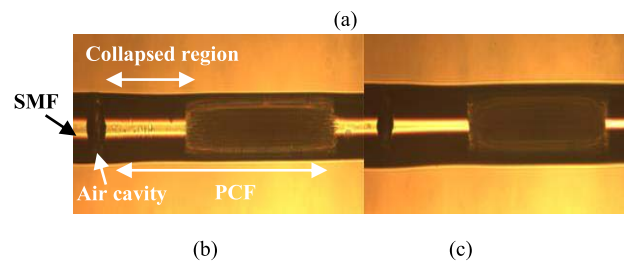
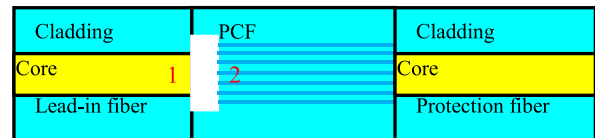


Fig. 1. (a) Schematic of the PCF FPI sensor. (b) Photo of the FPIs etched PCF FPI. (c) Photo of non-etched PCF FPI.

fiber [3]–[5], hollow-core photonic band-gap fiber and solid-core photonic crystal fiber (PCF) [7]–[9], chemical etching by cleaving and splicing [10], [11] and laser micromachining [12], [13]. We have demonstrated a method for constructing all-silica FPI sensors using 157nm laser micromachining [14]–[16].

In this paper, we report a self-enclosed Fabry–Perot air cavity created by splicing a single-mode fiber (SMF) to a PCF with a precise hole micro-machined by a 157nm laser at the end face of the PCF. The pressure and temperature coefficients of the FPI sensor were measured as  $\sim 39.3$  pm/MPa and  $\sim 0.9$  pm/°C, respectively, in a pressure range of 0–10MPa and temperature range of 25–700 °C. Furthermore, in order to enhance the pressure sensitivity and reduce temperature sensitivity, the fiber is etched to a diameter of  $\sim 96$   $\mu\text{m}$ . The enhanced pressure sensitivity is measured as  $\sim 54.7$  pm/MPa with a reduced temperature sensitivity of  $\sim 0.45$  pm/°C. The pressure responses of etched PCF FPI at different temperatures from room temperature to 700 °C are also measured, which shows good stability. These sensors have advantages in high temperature pressure measurement, such as good stability under high temperature, low cross-sensitivity of pressure to temperature, and easy of mass-production, etc.

## II. FABRICATION OF SELF-ENCLOSED FPI ON PCF

The configuration of the FPI on a PCF (TIR-PCF Changfei Co. Ltd, pure silicon single mode PCF) is given by Fig. 1(a). There is self-enclosed air cavity that is constructed on the

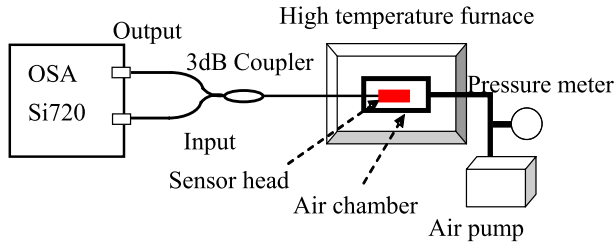


Fig. 2. Experimental setup of high-temperature and high-pressure test.

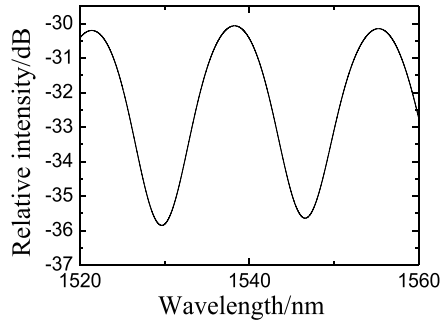


Fig. 3. Reflective spectrum of the self-enclosed FPI.

PCF spliced to two sections of SMFs, including two reflective surfaces indicated by 1 and 2 in Fig. 1. Such an air cavity could be used as a pressure sensing element due to its self-enclosed structure. It is fabricated by using following steps. We first made a circular hole with a depth of  $\sim 30\mu\text{m}$  and a diameter of  $\sim 60\mu\text{m}$  at the center of the cross section of the PCF by using a 157-nm laser micromachining system, which consists of a 157-nm pulsed laser (Coherent, LPF202), an optical focusing system (with 25 times demagnification), an observing system, and a precision translation stage. The pulse energy density, pulse width, and pulse repetition rate used were  $20\text{J}/\text{cm}^2$ , 15ns, and 20 Hz, respectively. 150 pulses were used to produce the hole, which took only 5 seconds. The hole is larger than the core but smaller than the cladding. Then, we spliced the PCF with hole and a cleaved SMF end to cover the hole, an air F-P cavity was formed with a length of  $\sim 45\mu\text{m}$ . The next, we cleaved the fiber with a short distance from the air cavity, and spliced it to another cleaved SMF to protect the PCF. From the structural mechanics, the pressure sensitivity of the air cavity could be enhanced by reducing the diameter of the fiber. Microscopic images of the fabricated sensors are shown in Fig. 1(b) and (c), respectively, for both etched and non-etched PCF FPIs.

The experimental setup is shown in Fig. 2. An optical spectrum analyzer (OSA) is used to measure the reflective spectrum of the sensor. The reflected spectrum of the sensor is measured and shown in Fig. 3.

### III. MATH HIGH-TEMPERATURE PRESSURE EXPERIMENT AND DISCUSSION

In our experiments, the sensor head was sealed into an air chamber and put into a high temperature furnace to perform pressure test at different temperatures. Experimental setup is shown in Fig. 2. Three FPI structures including PCF FPI,

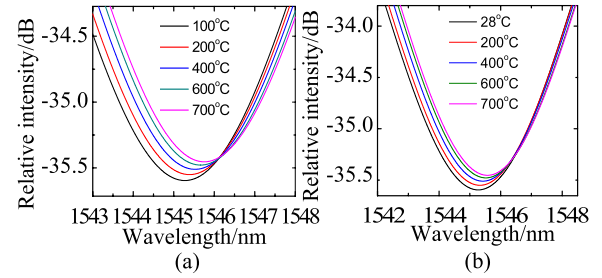


Fig. 4. Spectra of the FPIs at different temperatures. (a) Non-etched PCF FPI. (b) etched PCF FPI.

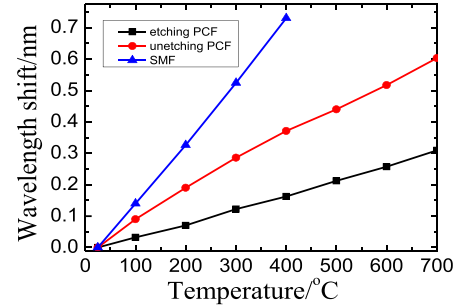


Fig. 5. Temperature responses of the three FPIs.

SMF FPI and etched PCF FPI, are used in high-temperature and high-temperature pressure tests. Here, a SMF FPI is constructed for comparison, which has a same structure as the PCF FPI except that the two fibers used for constructing FPI are all SMF. The diameter of SMF hole is also  $60\mu\text{m}$ , the fiber we used is high temperature coating SMF, with  $35\mu\text{m}$  cavity length. The original diameters of the SMF FPI and the PCF FPI were both  $125\mu\text{m}$ , in order to further enhance the pressure sensitivity, the PCF FPI was etched by HF acid to a diameter of  $\sim 96\mu\text{m}$ , corresponding to a reduction of  $\sim 14.5\mu\text{m}$  in wall thickness.

The temperature responses of the PCF FPI and etched PCF FPI are measured from  $25\text{ }^\circ\text{C}$  to  $700\text{ }^\circ\text{C}$  successively. The pit wavelength of the FPIs around  $1545\text{nm}$  shifts to longer wavelengths with the increase of temperature, as shown in Fig. 4. The temperature coefficients of the PCF FPI and etched PCF FPI are measured to be  $\sim 0.9\text{pm}/^\circ\text{C}$  and  $\sim 0.45\text{pm}/^\circ\text{C}$ , respectively, as shown in Fig. 5, corresponding to a temperature sensitivity decrease of 50% for the etched one. Additionally, The temperature response of the SMF FPI is measured in the range of  $25\text{ }^\circ\text{C}$  to  $400\text{ }^\circ\text{C}$  for comparison.

The temperature coefficient of the etched PCF FPI is much lower than the non-etched PCF FPI. The reason is that the thermal expansion of the fiber core would reduce the cavity length, while the thermal expansion of the remaining fiber cladding (the wall of the air cavity) would increase the cavity length [14]. When the thickness of the silica wall of the air cavity gets thinner, the force that the wall expanding the cavity is reduced, hence the thermal expansion effect of the cavity is effectively reduced. The temperature coefficient of SMF FPI is  $\sim 1.9\text{pm}/^\circ\text{C}$ , as shown in Fig. 6, which is much higher than that of the PCF FPI and etched PCF FPI.

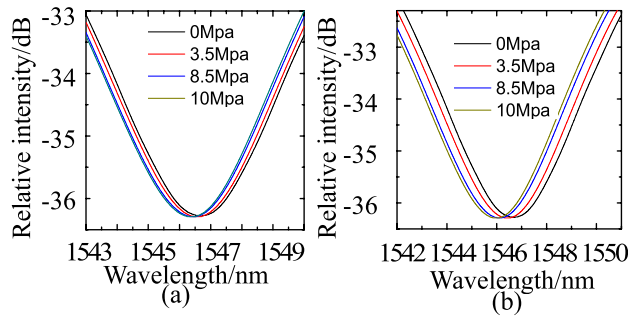


Fig. 6. Spectra of the PCF FPIs at different pressures. (a) Non-etched PCF FPI. (b) etched PCF FPI.

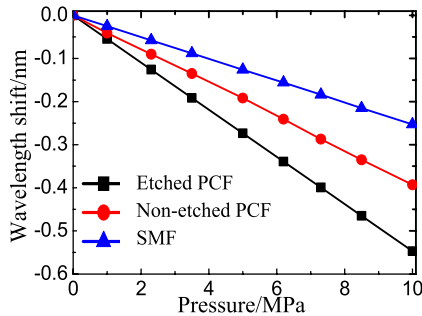


Fig. 7. Pressure responses of the three FPIs.

For SMF and PCF are made of the same material SiO<sub>2</sub> (the thermal expansion coefficient of SiO<sub>2</sub> is 0.55\*10<sup>-6</sup>m/K), the reason for the difference of temperature coefficients may be that the special air-hole structure of the PCF would weak the influence of the cladding expansion on core [17].

The pressure responses of the PCF FPI and etched PCF FPI are measured from 0 to 10MPa as shown in Fig. 6.

The pit wavelength of the FPI around 1545nm shifts to shorter wavelengths with the increase of pressure. The pressure coefficients of the PCF FPI and etched PCF FPI are measured as ~39.3pm/MPa and ~54.7pm/MPa, respectively, as shown in Fig. 7, corresponding to a pressure sensitivity enhancement of 40% for the sensor after etched. The pressure response of the SMF FPI is also measured in the range of 0 to 10MPa. The pressure coefficient is ~25.3pm/MPa, also as shown in Fig. 7, which is much lower than that of the PCF FPI and etched PCF FPI. Compared with the solid PCF FPI reported in [9], the sensitivity of the etched PCF FPI in this paper is ~10 times higher.

The reason for the pressure coefficient of the etched PCF FPI is higher than that of the non-etched one could be easily understood by equation (1) [18]:

$$\Delta\lambda = (\Delta L/L)\lambda_0 = [(1 - 2\mu)R_0^2P * \lambda_0]/E(R_0^2 - R^2) \quad (1)$$

where L is the effective cavity length of the air FPI on PCF, ΔL is the induced changes in L, λ<sub>0</sub> is a certain dip wavelength, R and R<sub>0</sub> are the effective radius of the air cavity and the radius of the fiber, respectively, E is Young’s modulus, μ is Poisson’s ratio, and P is the pressure applied. Compared with the SMF FPI, the air PCF FPI has relatively thin effective thickness R<sub>0</sub>–R, due to existence of the air hole, which leads to higher pressure sensitivity.

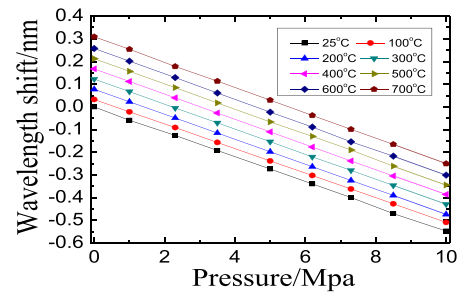


Fig. 8. Pressure responses of the etched PCF FPI at different temperatures.

The pressure responses of the etched PCF FPI at different temperatures are measured in the range of 0–10MPa, as shown in Fig. 8. During the test, it is found that the response of the etched PCF FPI shows good linearity and constant sensitivity at different temperatures, even up to 700 °C.

#### IV. CONCLUSION

The in-line PCF air cavity proposed in this paper could be operated under high temperature up to 700 °C. The pressure and temperature coefficients of the PCF FPI are measured to be 39.3pm/MPa and 0.9pm/°C, respectively. The pressure and temperature coefficients of the etched PCF FPI are 54.7pm/MPa and 0.45pm/°C, respectively. These sensors exhibit relatively high pressure sensitivity and low temperature sensitivity than those ever reported in-line solid PCF [9]. For high temperature pressure measurement, these PCF FPI sensors could offer two important valuable characteristics. The first is that they can stand for high temperature. The second is that they could offer relatively high pressure sensitivity and a low temperature coefficient to reduce cross-sensitivity. It is believed that these sensors could find important applications in harsh operation environments.

#### REFERENCES

- [1] Y.-J. Rao, “Recent progress in fiber-optic extrinsic Fabry–Perot interferometric sensors,” *Opt. Fiber Technol.*, vol. 12, no. 3, pp. 227–237, Jul. 2006.
- [2] B. Qi *et al.*, “Fiber optical pressure and temperature sensors for oil down hole applications,” in *Proc. SPIE*, vol. 4578, pp. 182–190, Feb. 2002.
- [3] X. Wang, J. Xu, Y. Zhu, K. L. Cooper, and A. Wang, “All-fused-silica miniature optical fiber tip pressure sensor,” *Opt. Lett.*, vol. 31, no. 7, pp. 885–887, Apr. 2006.
- [4] J. Xu, X. Wang, K. L. Cooper, G. R. Pickrell, and A. Wang, “Miniature temperature-insensitive Fabry–Pérot fiber-optic pressure sensor,” *IEEE Photon. Technol. Lett.*, vol. 18, no. 10, pp. 1134–1136, May 15, 2006.
- [5] H. Y. Choi, K. S. Park, S. J. Park, U.-C. Paek, B. H. Lee, and E. S. Choi, “Miniature fiber-optic high temperature sensor based on a hybrid structured Fabry–Perot interferometer,” *Opt. Lett.*, vol. 33, no. 21, pp. 2455–2457, Oct. 2008.
- [6] C. M. Jewart, Q. Wang, J. Canning, D. Grobncic, S. J. Mihailov, and K. P. Chen, “Ultrafast femtosecond-laser-induced fiber Bragg gratings in air-hole microstructured fibers for high-temperature pressure sensing,” *Opt. Lett.*, vol. 35, no. 9, pp. 1443–1445, Apr. 2010.
- [7] Y. J. Rao, T. Zhu, X. C. Yang, and D. W. Duan, “In-line fiber-optic etalon formed by hollow-core photonic crystal fiber,” *Opt. Lett.*, vol. 32, no. 18, pp. 2662–2664, Sep. 2007.
- [8] J. Villatoro, V. Finazzi, G. Coviello, and V. Pruneri, “Photonic-crystal-fiber-enabled micro-Fabry–Perot interferometer,” *Opt. Lett.*, vol. 34, no. 16, pp. 2441–2443, Aug. 2009.
- [9] C. Wu, H. Y. Fu, K. K. Qureshi, B.-O. Guan, and H. Y. Tam, “High-pressure and high-temperature characteristics of a Fabry–Perot interferometer based on photonic crystal fiber,” *Opt. Lett.*, vol. 36, no. 3, pp. 412–414, Jan. 2011.

- [10] Y. Zhu, K. L. Cooper, G. R. Pickrell, and A. Wang, "High-temperature fiber-tip pressure sensor," *J. Lightw. Technol.*, vol. 24, no. 2, pp. 861–869, Feb. 2006.
- [11] X. Chen, F. Shen, Z. Wang, Z. Huang, and A. Wang, "Micro-air-gap based intrinsic Fabry–Perot interferometric fiber-optic sensor," *Appl. Opt.*, vol. 45, no. 30, pp. 7760–7766, Apr. 2006.
- [12] S. Watson *et al.*, "Laser-machined fibers as Fabry–Perot pressure sensors," *Appl. Opt.*, vol. 45, no. 22, pp. 5590–5596, Feb. 2006.
- [13] T. Wei, Y. Han, H.-L. Tsai, and H. Xiao, "Miniaturized fiber inline Fabry–Perot interferometer fabricated with a femtosecond laser," *Opt. Lett.*, vol. 33, no. 6, pp. 536–538, 2008.
- [14] Z. L. Ran, Y. J. Rao, H. Y. Deng, and X. Liao, "Miniature in-line photonic crystal fiber etalon fabricated by 157 nm laser micromachining," *Opt. Lett.*, vol. 32, no. 21, pp. 3071–3073, Nov. 2007.
- [15] Z. Ran *et al.*, "Miniature fiber-optic tip high pressure sensors micromachined by 157 nm laser," *IEEE Sensors J.*, vol. 11, no. 5, pp. 1103–1106, May 2011.
- [16] Z. L. Ran, Y. J. Rao, H. Y. Deng, and X. Liao, "Self-enclosed all-fiber in-line etalon strain sensor micromachined by 157-nm laser pulses," *J. Lightw. Technol.*, vol. 27, no. 15, pp. 3143–3149, Aug. 1, 2009.
- [17] P. Russell, "Photonic crystal fibers," *Science*, vol. 299, no. 5605, pp. 358–362, Jan. 2003.
- [18] Z. Ran, Y. Rao, J. Zhang, and B. Xu, "Laser-machined all-fiber in-line tip pressure sensor," *Proc. SPIE*, vol. 7503, pp. 75032X-1–75032X-2, Mar. 2009.

**Shan Liu**, photograph and biography not available at the time of publication.

**Qin Liu**, photograph and biography not available at the time of publication.

**Yanjun Wang**, photograph and biography not available at the time of publication.

**Haihong Bao**, photograph and biography not available at the time of publication.



**Zengling Ran** was born in Chongqing, China, in 1977. He received the M.Eng. degree from the Department of Optoelectronic Engineering, Chongqing University, Chongqing, in 2003, and the Ph.D. degree from the University of Electronic Science and Technology of China, Chengdu, China, in 2009, where he is currently a Professor with the Key Laboratory of Optical Fiber Sensing and Communications, Ministry of Education. His current research interests include fiber-optic sensing and optical fiber transmission technology.



**Yunjiang Rao** was born in YunNan, China, in 1962. He received the M.Eng. and Ph.D. degrees from the Department of Optoelectronic Engineering, Chongqing University, China, in 1986 and 1990, respectively. He is the Supervisor of the Key Laboratory of Optical Fiber Sensing and Communications (Ministry of Education), University of Electronic Science and Technology of China. His current research interests are optic fiber technology and optoelectronic devices.